EUROPEAN ORGANIZATION FOR NUCLEAR RESEARCH
CERN - ACCELERATORS AND TECHNOLOGY SECTOR

CERN-ATS-2012-050

Design and Development of Separation Septa for the CERN PS Booster Upgrade

B. Balhan, J. Borburgh, M. Hourican, T. Masson
CERN, Geneva, Switzerland

Abstract

The CERN PS Booster project foresees the injection of 160 MeV H- ions into the booster from Linac 4. For this substantial upgrade, a system of 5 pulsed magnets (BIDIS) and 3 vertical septa (BISMV) will distribute the Linac pulses into the four-vertically separated Booster injection lines before being injected into the rings. This paper describes the magnetic calculations and the design concept that will be used in the future upgrade of the BISMV. Subsequently the mechanical design of the septa and their integration into the existing transfer line will be discussed.

Presented at the 22nd International Conference on Magnet Technology (MT-22)
12-16 September 2011, Marseille, France

Geneva, Switzerland

February 2012

Design and Development of separation septa for the CERN PS Booster upgrade

B. Balhan, J. Borburgh, M. Hourican, T. Masson

***Abstract*—The CERN PS Booster project foresees the injection of 160 MeV H^- ions into the booster from Linac 4. For this substantial upgrade, a system of 5 pulsed magnets (BIDIS) and 3 vertical septa (BISMV) will distribute the Linac pulses into the four-vertically separated Booster injection lines before being injected into the rings. This paper describes the magnetic calculations and the design concept that will be used in the future upgrade of the BISMV. Subsequently the mechanical design of the septa and their integration into the existing transfer line will be discussed.**

***Index Terms*— vertical deflecting septa, vacuum tank.**

I. INTRODUCTION

As part of the upgrade project for the transfer line from the Linac4 to the PS Booster, the vertical deflecting septa will be replaced. The original ferrite septa cannot cope with the increase in beam energy from 50 to 160 MeV so a new set of magnetic laminated septa have been designed. The pulsed septa, based on conventional design technology, will operate under vacuum, be bakeable, and will be used to distribute the beam to each of the 4 booster superimposed rings.

II. BEAM TRAJECTORIES

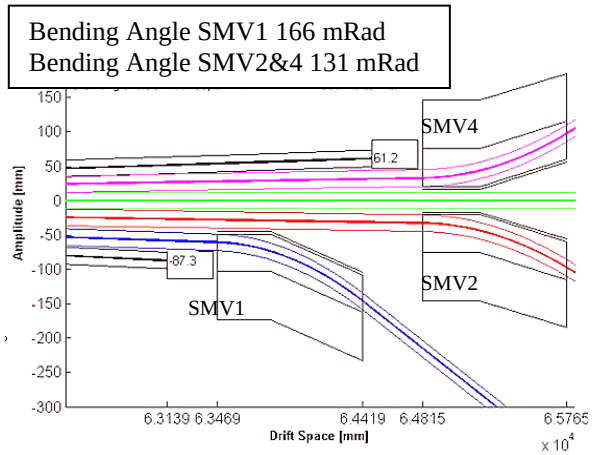

Fig. 1. The beam trajectories (coloured tracks) and deflections at the BISMV. The Head and Tail dump can absorb the rising and falling edge (black tracks) of the Linac beam in case of chopper failures.

Manuscript received 12 September 2011.
B. Balhan, J. Borburgh, M. Hourican, T. Masson are with the TE Department in CERN, Geneva, Switzerland. (Phone: +4122 7678241, e-mail: Michael.Hourican@cern.ch).

The septum vacuum tank will also house the so-called head and tail dumps for absorbing the rising and falling edges of the Linac4 beam, in case the chopper upstream in the Linac has not removed them already at lower energy.

A. Vertical deflections for 4 rings

A fast distributor (BIDIS) initially deflects the 6 time resolved slices of the Linac4 beam in order that they enter the BISMV with varying angles. The initial slice (head) is deflected immediately to the head dump and similarly the last slice is deflected to the Tail dump. Of the remaining 4 slices of beam, one slice passes straight through the tank and enters ring 3 of the Booster; the other 3 slices are deflected to the other remaining rings of the Booster. SMV1 deflects the beam by 160 mrad to ring 1 and SMV 2 and 4 deflect through 130 mrad to rings 2 and 4 (Fig. 1).

B. Proposed Solution

The current BISMV comprises 3 ferrite cored septum magnets housed in an “Omega” section vacuum tank. Due to the increased beam energy these need to be replaced with laminated steel magnets to allow for higher field strengths. At the same time the vacuum tank will be replaced with a modular, circular section, UHV compatible system. This will allow for shorter intervention times in the event of failures or preventive maintenance. The vacuum tank incorporates the septa and the Head and Tail dumps. In Fig. 1 the 3 deflected beams and one non deflected beam (in green) are highlighted. Each beam is deflected using a pair of identical septum magnets connected in series with its own dedicated power supply. The current, hence the beam angle, can be varied to optimize the beam acceptance and to minimize the losses.

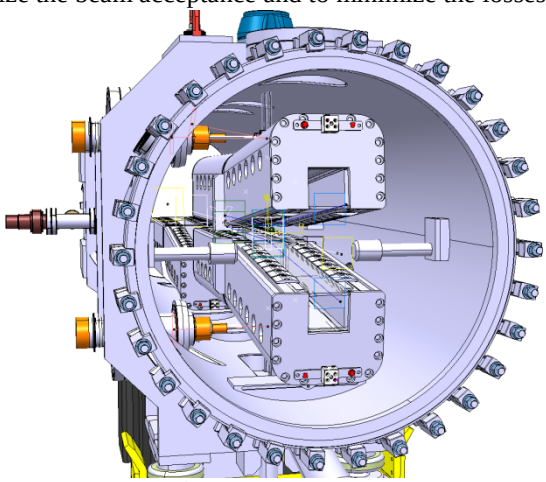

Fig. 2. The internal layout of magnets and power connections.

Each magnet pair is rigidly fixed together with a given angle which is optimized to closely follow the deflected beam path and maximize the vertical beam acceptance.

Each pair of magnets is fitted with a high current UHV feedthrough rated at 34 kA and with its own individual water circuit to cool the magnets. The two magnets per beam are connected electrically in series and cooled in parallel.

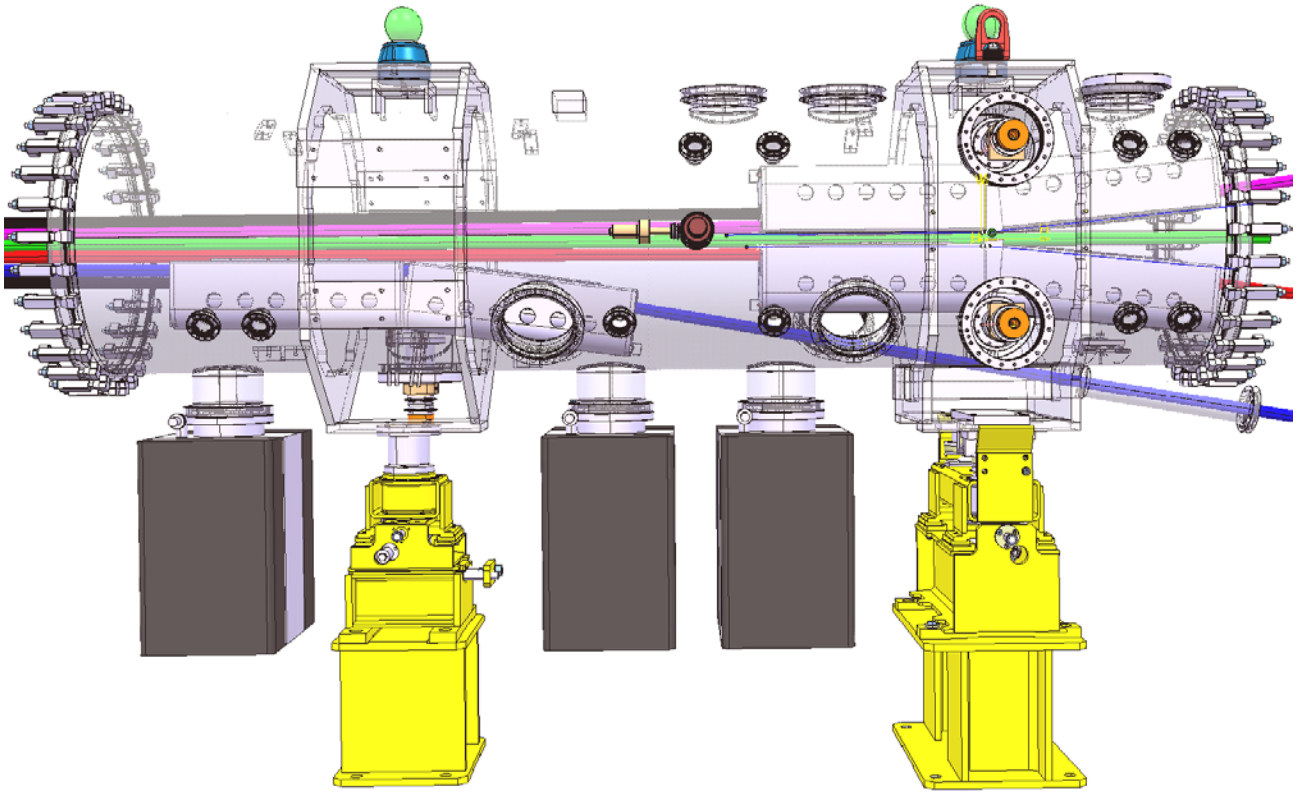

Fig. 3. Complete system showing the septum magnet in the vacuum vessel. The coloured tracks represent the trajectories of the four booster beams.

TABLE 1 PRINCIPAL SEPTUM PARAMETERS

Parameter	Value
Kinetic Energy	160 MeV
Particle deflection	173 mrad
Gap height/width	70x69 mm
Length Magnetic/physical	960 / 1050 mm
Yoke H / W	150 / 120 mm
∫Bdl	0.329 T.m
Peak Current / Induction in gap	19.1 kA / 0.343 T
Inductance / turns	1.22 µH / 1
Septum / Rear conductor thickness	4.5 / 10 mm
Rise time / rep. rate / flat top	0.1 / 0.9 /1 ms
Magnet R / Power dissip.	~ 0.2 mΩ / 40 W

III. MAGNET SIMULATIONS

Following the decision to build the magnets using two separate magnet blocks, the design focus was on maximizing the magnetic length for the given space available, while keeping the leakage field as low as possible. The magnets have been modeled using Opera® 3D software from Cobham. The first challenge was to perform simulations using two identical magnets in order to limit developments and realization costs, the optimization of the angle and the offset between magnets was done with these limitations.

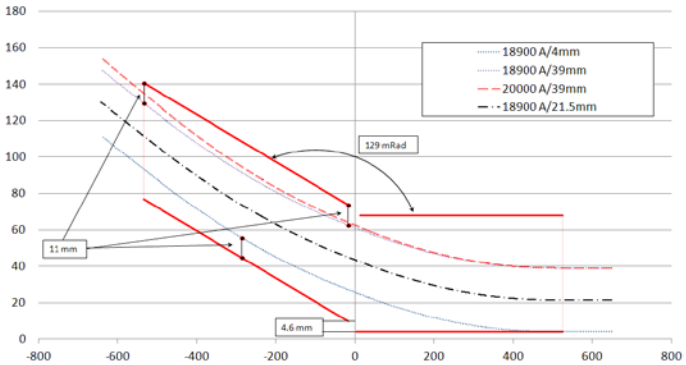

Fig. 4. Optimization of magnet positioning using the simulation results for the beam trajectory.

The field is maintained inside the magnet using field clamps made of soft steel (Armco) at the entrance and exit of the magnet stack; the end plates used to clamp the magnets near

the stack centre are made of stainless steel to maximize the magnetic length and hence keep the current as low as possible. This design improvement provided an increase of 9 mm in the magnetic length.

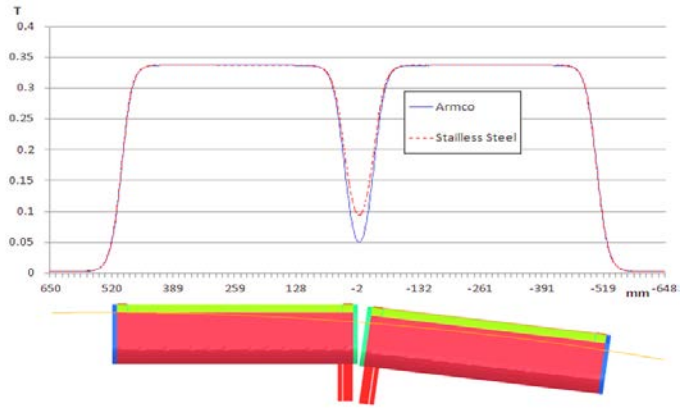

Fig. 5. Magnetic flux density (Bmod) along extracted beam axis with different middle plates materials.

The resulting leakage field from the void between the 2 magnets was analyzed to assess the effect on the deflected beams. The effect of the stainless steel mid plates is relatively low and negligible; the magnetic measurement on the prototype should allow confirmation of this.

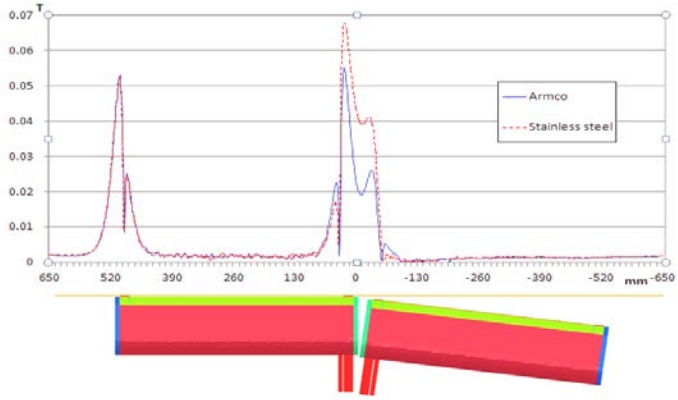

Fig. 6. Maximum leakage field parallel to the “circulating beam” axis (2 mm from the septum) with different middle plates materials.

A first 2D analysis has been performed to estimate the leakage field, but since the leakage field is dominated by the extremities of the stack we finally use the integral value. These values were extracted to perform field homogeneity analysis for B_y and B_{mod} components. The results of the simulations are presented in the figures below; the values are expressed as a % of $B_{nominal}$ on the mid plane of the magnet on the centre axis.

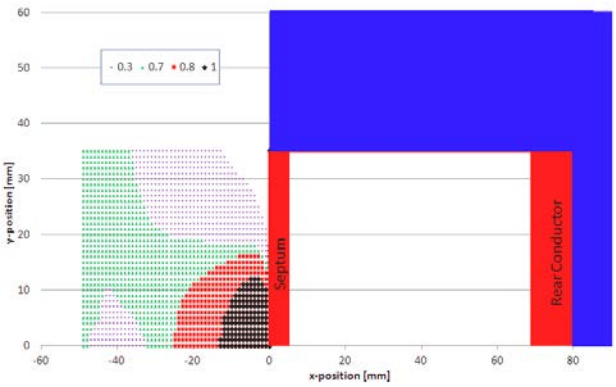

Fig. 7. Integrated leak field, expressed as %age of nominal gap field, parallel to the septum blade at indicated positions (x,y positions) based on By integral values.

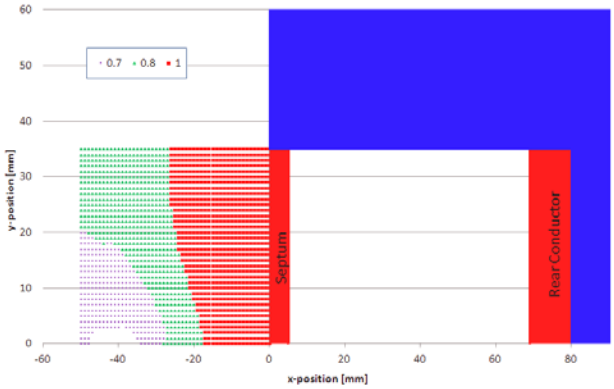

Fig. 8. Integrated leak field, expressed as %age of nominal gap field, parallel to the septum blade at indicated positions (x,y positions) based on Bmod integral values.

Note: B_{mod} takes into account the magnitude B_y and B_x components of the field which accounts for the difference in fig. 7 and fig. 8.

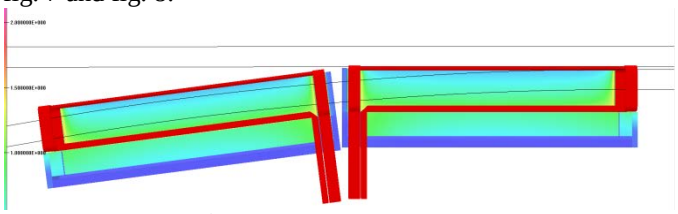

Fig. 9. Superposition of the ejected and non-ejected beam trajectory using the results of the field mapping simulation.

In the figure above the optimization of the magnet position allows for the centering of the beam in the gap. The maximum value of the power supply current has been used for the tracking in order to assess the minimum clearance between the coil extremities and extracted beam at this maximum deflection.

IV. Mechanical Design

The magnets will be constructed using laminations of 0.35 mm thick non-oriented electrical steel, type M330-35A which have been pre-coated with an inorganic insulation with some organic components (Stabolit 20). The laminations shall be compressed and maintained using stainless steel and Armco end plates at opposite ends. The coil is of a brazed construction and incorporates a thin walled cooling tube (stainless steel diameter 2.5/2 mm) in the septum and a copper

tube with a 4 mm hole in the rear conductor. The assembly of the individual magnets is performed according to a specific procedure. The individual laminations are stacked and clamped rigidly, followed by insertion (and adjustment if necessary) of the coil. A twin magnet support structure is then used to align two septa together on a precision alignment table. The high current feedthrough is then fitted to the magnets and the cooling circuit connections brazed. A major improvement in the design is that the final brazing of the feedthroughs can now be carried out in the laboratory before inserting the magnets in the vacuum tank. Previously the final braze was carried out after insertion of the magnets in the vacuum tank and in difficult conditions due to space limitation around the feedthrough port. This braze is the most critical and has to be 100% leak tight. The magnets are then connected in series using copper interconnects and the complete assembly is adjusted to the corresponding angle. When the alignment has been verified the complete stack assembly is then inserted into the vacuum chamber and the external survey targets are used to do the final alignment. The procedure for the downstream magnets is to insert the lower magnet stack in to its “park” position, followed by insertion of the upper stack. The lower stack is then moved to the nominal position. When the lower stack has been secured the upper stack is positioned on the same support and nominal alignment is then verified. A dedicated lifting apparatus has been foreseen to perform all of the insertion procedure under laboratory conditions.

The septum blade is the most stressed component; it has been analyzed for stress distribution during the 20 kA pulse.

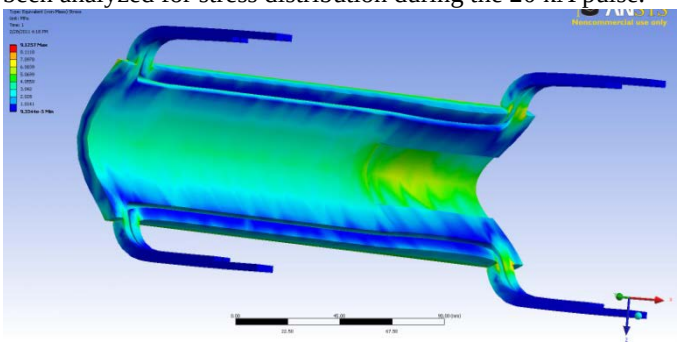

Fig. 10 Stress distribution in the septum blade.

The magnitude of the stress intensity in the vicinity of the crossover legs at the start of the bend (Figs. 10) is 9.1 MPa and is well within the maximum allowable stress for the material used. The coil will be manufactured from Copper (OFE) and the maximum allowable stress in the untreated material is 195 MPa. However, since the coil is brazed in a vacuum furnace it goes through an annealing cycle and the maximum allowable stress is significantly reduced to values in the range of 40-50 MPa. Following fatigue analysis, a minimum factor of safety of 15 has been estimated. The estimated maximum deformation of the septum blade is in the order of 0.005 mm. The magnets are each equipped with an integrated heating element, UHV compatible and capable of heating each magnet to the required 200 C. A thermal analysis has been carried out to assess the temperature distribution in the assembly; the result is shown in Fig. 11. The main mode of heat transfer is by conduction through the stainless steel support with approximately 10-15 % of radiant effect from the element to the laminations.

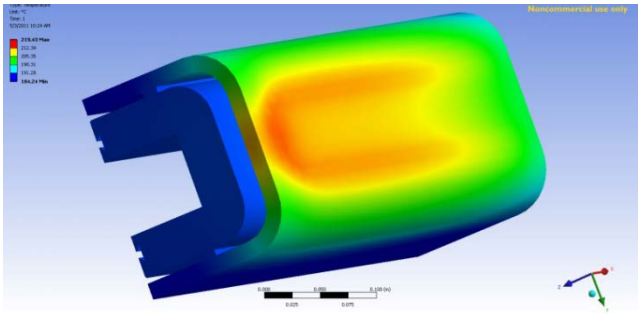

Fig. 11. Temperature distribution in the magnet yoke support.

V. Vacuum Pumping

A target pressure in the 10^{-9} mbar range is reached using three 400 l/s ion pumps and baking out of the magnets prior to operation. A primary turbo pumping group shall be used during bake outs when gas load will be at a maximum. A major determining factor in downtime following a failure and venting of the laminated septa is the high thermal inertia of the magnet yokes. The time required to cool the magnets from 200 ºC to about 50 ºC can be significant and during this time the gas load is high. The turbo molecular pump will significantly boost the pumping capacity of this sector during these bake-out cycles. The power for the bake-out, 500 W per magnet, is provided by heating elements fitted to each magnet support.

VI. Conclusion

The required increase in field strength is achieved by replacing the ferrite magnets with laminated steel magnets which are well below their saturation levels.

By using the results of the particle tracking simulation it has been possible to design a magnet with a reduced gap width. Optimization of the relative position of each magnet has been made possible and this allows the beam to pass through the best field region of the magnet. The magnets have been positioned such that the clearance between the beam and the yoke/coil at exit and entry has been maximized.

The “Omega” shaped vacuum tank is replaced with a circular section vacuum tank to improve the operating pressure. A failure in the system will involve relatively short intervention times due to the fact that the complete tank/magnet assembly can be replaced in a matter of hours. The duration of the intervention will be mainly determined by the amount of time required to reach operational vacuum levels.

The magnets are all identical which allows for reduced amount of tooling and spares.

References

[1] F. Gerigk, M. Vretenar (eds.), “Linac4 Technical Design Report”, CERN-AB-2006-084.

[2] J. Borburgh et al., “Septa and distributor developments for H- injection into the Booster from Linac4”, EPAC’08, Genoa

[3] J. Borburgh et al, “160 MeV H^- Injection into the CERN PSB”, Proceedings of PAC07, TUPAN109, Albuqquerque, New Mexico, USA.

[4] M. Thivent et al, “A new set of Magnetic Septa in the Cern PS complex”, Proceedings of the 1999 Particle Accelerator Conference, New York, USA.